IJMMM International Journal of Minerals, Metallurgy and Materials 矿物冶金与材料学报（英文版）

Evolution of ferronickel particles during the reduction of low-grade saprolitic laterite nickel ore by coal in the temperature range of 900–1250°C with the addition of $CaO–CaF_2–H_3BO_3$

Zulfiadi Zulhan and Windu Shalat

Cite this article as:
Zulfiadi Zulhan and Windu Shalat, Evolution of ferronickel particles during the reduction of low-grade saprolitic laterite nickel ore by coal in the temperature range of 900–1250°C with the addition of $CaO–CaF_2–H_3BO_3$, *Int. J. Miner. Metall. Mater.*, 28(2021), No. 4, pp. 612-620. https://doi.org/10.1007/s12613-020-2025-0

View the article online at SpringerLink or IJMMM Webpage.

International Journal of Minerals, Metallurgy and Materials
Volume 28, Number 4, April 2021, Page 612
https://doi.org/10.1007/s12613-020-2025-0

Evolution of ferronickel particles during the reduction of low-grade saprolitic laterite nickel ore by coal in the temperature range of 900–1250°C with the addition of $CaO–CaF_2–H_3BO_3$

Zulfiadi Zulhan[*] *and Windu Shalat*[*]

Metallurgical Engineering Department, Faculty of Mining and Petroleum Engineering, Bandung Institute of Technology, Indonesia
(Received: 30 December 2019; revised: 8 February 2020; accepted: 17 February 2020)

Abstract: The method of producing ferronickel at low temperature (1250–1400°C) has been applied since the 1950s at Nippon Yakin Kogyo, Oheyama Works, Japan. Limestone was used as an additive to adjust the slag composition for lowering the slag melting point. The ferronickel product was recovered by means of a magnetic separator from semi-molten slag and metal after water quenching. To increase the efficiency of magnetic separation, a large particle size of ferronickel is desired. Therefore, in this study, the influences of CaO, CaF_2, and H_3BO_3 additives on the evolution of ferronickel particle at ≤1250°C were investigated. The experiments were conducted at 900–1250°C with the addition of CaO, CaF_2, and H_3BO_3. The reduction processes were carried out in a horizontal tube furnace for 2 h under argon atmosphere. At 1250°C, with the CaO addition of 10wt% of the ore weight, ferronickel particles with size of 20 μm were obtained. The ferronickel particle size increased to 165 μm by adding 10wt% CaO and 10wt% CaF_2. The addition of boric acid further increased the ferronickel particle size to 376 μm, as shown by the experiments with the addition of 10wt% CaO, 10wt% CaF_2, and 10wt% H_3BO_3.

Keywords: saprolitic laterite nickel ore; ferronickel particle; lime; fluorite; boric acid

1. Introduction

Nickel is an important metal widely used in daily life. Nickel has relatively low thermal and electrical conductivity, high corrosion resistance, high strength, and excellent toughness. Nickel is primarily used in the form of ferroalloy for the manufacture of stainless steel (78%); around 10% of nickel is for nickel-based alloy applications, about 4% of nickel is for plating, and 8% of nickel is for other applications including batteries, coins, and nickel chemicals [1]. In 2018, global nickel metal resources in nickel ores were estimated to contain at least 130 million tons of metal with an average nickel content of 1wt%. This resource consists of 60% ore with laterite type and 40% with sulfide. Currently, almost 60% of nickel production comes from sulfide-type nickel ore [2].

Lateritic nickel ore can be processed via hydrometallurgy and/or pyrometallurgy. In general, saprolitic laterite nickel ore is processed by pyrometallurgy and limonite is processed by hydrometallurgy. Through pyrometallurgy, there are three proven technologies for the processing of saprolitic laterite nickel ore, namely, RKEF (rotary kiln–electric furnace), blast furnace, and Krupp–Renn. Among these technologies, RKEF is the most popular due to its capability to melt the refractory type of ferronickel slag consisting mainly of silica and magnesia. RKEF is mature technology that is extensively applied across the world for the processing of saprolite-type lateritic nickel ore to produce nickel metal in the form of ferronickel, nickel matte, or nickel pig iron. High energy consumption and high capital expenditure are the limitations of ferronickel production via RKEF. Therefore, an alternative lateritic nickel ore processing route, which has low energy consumption, low operational cost, and low capital cost, is warranted. One method to address this challenge is to reduce laterite nickel ore at moderate temperatures to form ferronickel particles [3]. These ferronickel particles can then be physically separated using a magnetic separator. The effectiveness of this process is highly dependent on the ease of separation of ferronickel particles from the unreduced oxides in the ore. The ease of separation of particles is highly dependent on the particle size of the ferronickel particles. Large particles will separate easily from surrounding impurities.

Harris *et al.* [3] and Dong *et al.* [4] summarized the

*These authors contributed equally to this work.

Corresponding author: Zulfiadi Zulhan E-mail: zulfiadi.zulhan@gmail.com

thermal upgrading of nickeliferous laterites by using additives. Most of the research in the literature added sulfur-containing additives to increase the size of ferronickel [5–14]. Li *et al.* [5] added 20wt% sodium sulfate and coal into saprolite-type lateritic nickel ore and reported that the ferronickel particle size increased from 5 to 10 μm to approximately 50 μm at 1100°C due to the presence of troilite (FeS) as an activating agent to facilitate the aggregation of ferronickel particles. Similar experiments were conducted by Zhu *et al.* [6], where 6wt% calcium sulfate was added into nickel ore and coal at 1100°C to produce ferronickel particle with the size of 16.1 μm. The effect of elemental sulfur and pyrite addition into limonite nickel ore using coal as a reductant on the ferronickel particle formation was investigated by Elliott *et al.* [8]. In general, the addition of sulfur-containing additives increases the sulfur content in the ferronickel product, which requires a high amount of desulfurizing agents during stainless steel production. By contrast, high sulfur content in ferronickel has the benefit of producing pure nickel, where iron and nickel in iron–nickel sulfide can be easily separated. Other additives are chloride-based ones, such as sodium chloride and calcium chloride. Zhou *et al.* [15] used sodium chloride and coal in high-magnesium, low-nickel lateritic ore and found that the nickel recovery increased to 98.31% at 1200°C. However, the utilization of a chloridizing agent (Cl_2, NaCl, and $CaCl_2$) for processing of lateritic nickel ore leads to heavy environmental pollution [16].

Lime in the form of limestone was used as an additive for Krupp–Renn rotary kiln process at Nippon Yakin Kogyo, Oheyama Works, Japan, since 1952 to produce ferronickel luppen at 1250–1400°C [17–18]. The particle size of ferronickel luppen is between 0.5 and 20 mm, with the average size around 1 mm [19–20]. The amount of limestone addition for ferronickel luppen production was not reported due to confidentiality. Li *et al.* studied the effect of CaO addition in the reduction of low-grade saprolite-type nickel laterite ore and found that the optimum CaO addition is around 10wt% [21]. Besides lowering the melting point of slag, CaO has an important role in replacing NiO that is bound by SiO_2 in olivine. This phenomenon was proposed as the alkaline oxide effect ($CaO + 2NiO{\cdot}SiO_2 = CaO{\cdot}SiO_2 + 2NiO$) [21]. Lv *et al.* [22] adjusted the quaternary basicity [$(m_{CaO} + m_{MgO})/(m_{SiO_2} + m_{Al_2O_3})$], where m is mass fraction, by adding CaO into nickel laterite ore, and they reported a nickel content of 11.53wt% in ferronickel and 98.59% of nickel recovery. Similar results of the influence of CaO addition on nickel grade in ferronickel and nickel recovery were reported by other studies [16,23].

The effect of borax was studied by Morcali *et al.* [24] for the extraction of Ni and Co from limonitic laterite ore. They reported that Ni–Co–Fe matte can be produced at 1000°C by adding up to 12.7wt% of borax together with sodium carbonate. The presence of sulfur further enhances the nickel and cobalt recoveries. The nickel and cobalt recoveries of 98% and 95% were achieved by the addition of 108wt% flux mixture ($50wt\%Na_2CO_3 + 35wt\%Na_2B_4O_7{\cdot}10H_2O + 15wt\%SiO_2$), 3.2wt% coke, and 20wt% elemental sulfur into roasted limonitic laterite ore.

In this paper, we investigated the influences of lime (CaO), fluorite (CaF_2), and boric acid (H_3BO_3) as a source of borax in the slag on the evolution of ferronickel particle. The aim of these additions was to determine alternative combinations of fluxes to increase the size of ferronickel particles, thereby enhancing its separation from the unreduced oxides and lowering the operating temperature for ferronickel production.

2. Experimental

The lateritic nickel ore was low-grade saprolite ore (LGSO) originating from Sulawesi Island, Indonesia. Before being used in the experiment, the saprolitic nickel laterite ore was dried at 135°C for 24 h, ground by using a ball mill, and sieved to obtain the grain size of less than 65# (−210 μm). The chemical composition of nickel ore, which was determined by X-ray fluorescence (XRF), is given in Table 1. The results of X-ray diffraction (XRD) analysis are shown in Fig. 1, which indicates that the nickel laterite ore consisted mainly of lizardite/antigorite and quartz.

Table 1. Chemical composition of saprolitic nickel ore wt%

Ni	Fe	Si	Mg	Al	Cr	Ca	Mn	LOI
1.31	8.3	20.79	15.04	1.69	0.414	0.395	0.178	10.14

Note: LOI—loss on ignition.

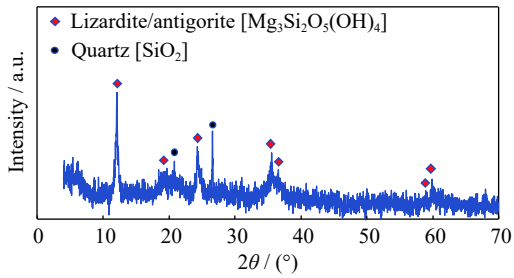

Fig. 1. XRD spectra of saprolitic nickel ore.

Coal as a reductant was crushed using a roll mill, ground in a ball mill, and sieved to obtain a grain size of less than 65# (−210 μm). The coal was then dried at 135°C for 24 h to remove moisture. The results of proximate and ultimate analyses of coal are shown in Tables 2 and 3, respectively. The CaO (pro analysis), H_3BO_3 (pro analysis), and CaF_2 (technical grade) additives were ground and sieved so that a size fraction of less than −80# (−177 μm) was obtained. The chemical composition of CaF_2, which was analyzed by XRF, is lis-

ted in Table 4. These additives/fluxes were dried in an oven at 135°C for 24 h.

Table 2. Coal proximate analysis (air dry basis) wt%

Moisture	Ash	Volatile matter	Fix carbon
1.93	17.47	35.21	45.39

Table 3. Coal ultimate analysis (air dry basis) wt%

C	S	H	N	O
64.13	0.92	3.94	1.24	12.3

Table 4. Chemical composition of CaF_2 technical grade wt%

CaF_2	Fe_2O_3	Al_2O_3	SiO_2
97.21	0.93	0.66	1.2

The saprolitic nickel laterite ore was mixed with coal and additives and formed into briquettes by using a hydraulic press machine at a load of 5 t. Three mixtures of briquette were prepared: briquettes A, B, and C. Briquette A consisted of 3 g of nickel ore as basis with the addition of 10wt% coal and 10wt% CaO of the ore weight. Briquette B comprised 3 g of nickel ore as basis mixed with 10wt% coal, 10wt% CaO, and 10wt% CaF_2. Briquette C was prepared by mixing 3 g of nickel ore with the addition of 10wt% coal, 10wt% CaO, 10wt% CaF_2, and 10wt% H_3BO_3. Details of the mixture containing nickel ore, coal, and additives are provided in Table 5.

Table 5. Different nickel ore, coal, and additives mixtures used in this work g

Briquette	Ore	Coal	CaO	CaF_2	H_3BO_3
A	3	0.3	0.3	—	—
B	3	0.3	0.3	0.3	—
C	3	0.3	0.3	0.3	0.3

The diameter of the briquettes was 15 mm, and the height was in the range of 1.04–1.27 mm. The experiments for the reduction of nickel ore by coal with the addition of fluxes were conducted in a horizontal tube furnace under argon gas atmosphere with the flow rate of 1 L/min at 900, 1000, 1100, 1150, 1200, and 1250°C for 2 h. Three briquettes from each mixture were placed into an alumina crucible. After the target temperature of the tube furnace was achieved, argon was allowed to flow for 3 min prior to the insertion of the briquettes into the furnace to remove the air inside the tube so that the inert conditions were achieved. After the reduction process was completed, the briquettes were removed from the tube furnace and cooled to room temperature in a desiccator to avoid the re-oxidation of the formed ferronickel. The reduced briquette was weighed, documented, and analyzed by optical microscopy and scanning electron microscopy–energy dispersive X-ray spectroscopy (SEM–EDS). The particle sizes were analyzed by ImageJ software, which is an open source image processing program.

3. Results and discussion

3.1. Thermodynamics analysis

The influences of CaO, CaF_2, and H_3BO_3 additives on the reduction of saprolitic nickel laterite ore with chemical composition given in Table 1 were evaluated using the Equilib module in FactSage 7.1 thermodynamic software using the FToxid and FTmisc databases. The amount of carbon added was 5wt%, and the amount of additives was based on the mixtures in briquettes A, B, and C. The output of the calculations was the compositions and amounts of gas, slag, solid oxides, and metal phases at equilibrium. At temperature ≤ 1250°C, the ferronickel smelting slag is in solid state, so the influence of additive on the formation of the liquid phase in the slag was observed. During the reduction of the briquette, the formed ferronickel particles could easily migrate, merge, agglomerate, and grow in the molten phase compared with those in the solid phase.

Fig. 2 shows the calculated liquid proportion in the slag in the temperature range of 900–1250°C for briquettes A, B, and C. By adding 10wt% CaO as additive in dry saprolitic nickel laterite ore (briquette A), liquid slag was formed at 1250°C with the proportion of 15wt%. No liquid slag was present at 900–1200°C. The solid slag consisted of clinopyroxene and olivine. In briquette B, on the addition of 10wt% CaO and 10wt% CaF_2, liquid slag started to exist at 1000°C with the amount of 4.5wt%. The proportion of liquid slag increased as the temperature rose, and 66.7wt% was achieved at 1250°C. The solid mineral at 1250°C was olivine. The influence of boric acid (H_3BO_3) was studied in briquette C where the additives consisted of 10wt% CaO, 10wt% CaF_2, and 10wt% H_3BO_3. The tendency of briquette C was similar to that of briquette B where liquid slag was formed at 1000°C. In terms of the amount of liquid slag, briquette C had a higher proportion of liquid slag than briquette B in the temperature range of 1000–1150°C but with a lower proportion of liquid slag than briquette B at $T \geq 1200$°C. In

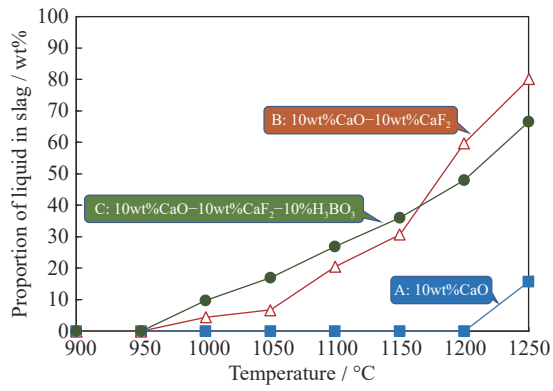

Fig. 2. Proportion of liquid in the slag as a function of temperature and flux at 5wt% carbon addition based on FactSage calculation.

general, the additions of CaF_2 and H_3BO_3 into the slag increased the amount of liquid phase in the slag compared with the addition of CaO alone. The high proportion of the liquid phase in the slag assisted the agglomeration of metal particles.

The thermodynamics calculation revealed that the nickel recoveries in briquettes A, B, and C were 100% due to the excess of carbon as reductant. However, the iron recovery and nickel content in ferronickel in each briquette differed (Fig. 3). The figure shows that the ratio of Ni/Fe in ferronickel was higher at lower temperature than at higher temperature, because nickel oxide was easier to be reduced than iron oxide at low temperature. The addition of H_3BO_3 increased the Ni/Fe ratio in ferronickel, which indicated that a high nickel content in ferronickel was achieved and the reduction of iron oxide was suppressed.

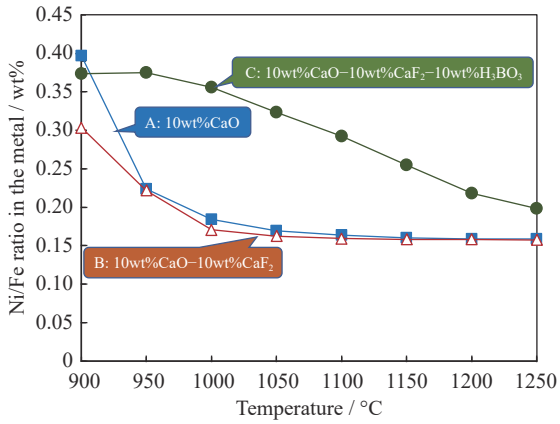

Fig. 3. Ratio of Ni/Fe in the ferronickel as a function of temperature and flux at 5wt% carbon addition based on FactSage calculation.

The stability of boric acid as function of temperature based on FactSage calculation is depicted in Fig. 4. Boric acid (H_3BO_3) was dissociated into HBO_3(s) and H_2O(g) at temperatures (T) higher than 100°C. In the range of 300–450°C, B_2O_3(s), $(HBO_2)_3$(g) and H_3BO_3(g) were formed. At T > 450°C, B_2O_3(s) solid was converted into B_2O_3(l) because the melting point of B_2O_3 is 450°C. The presence of B_2O_3 liquid in the slag lowered the melting point and viscosity of the slag, which facilitated the agglomeration and growth of metal particles.

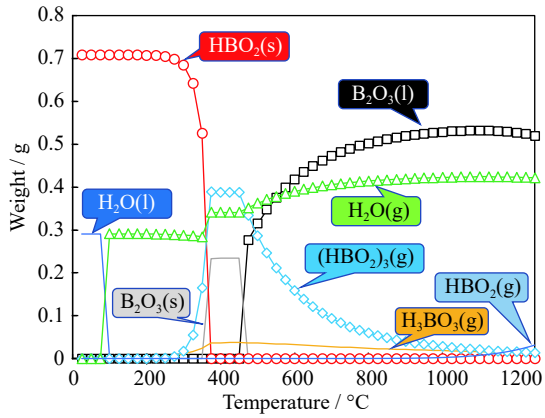

Fig. 4. Stability of boric acid as function of temperature based on FactSage calculation.

3.2. Visual observation and weight loss

The photographs of the briquettes after the reduction are shown in Fig. 5. For briquette A with the addition of 10wt% CaO, the deformation of briquette was observed at 1250°C. At 900–1200°C, the briquettes appeared to be in a solid state. These results were in line with the thermodynamics calculation (Fig. 2), where the proportion of liquid phase in the slag was 15wt% at 1250°C and no liquid slag was formed at 900–1200°C. By contrast, briquettes B and C were already deformed at 1200 and 1150°C, respectively. These phenomena were also in agreement with the thermodynamics calculations shown in Fig. 2, where the slag liquid was readily formed at 1000°C.

After the reduction, weight loss of the briquette was observed (Fig. 6). Weight loss was due to the evaporation of bound water, release of volatile matter and inherent moisture in coal, and reduction of oxygen in metal oxides (iron oxide, nickel oxide, and chromium oxide) by carbon in coal, thereby forming CO or CO_2 gas. The percentage of weight loss from

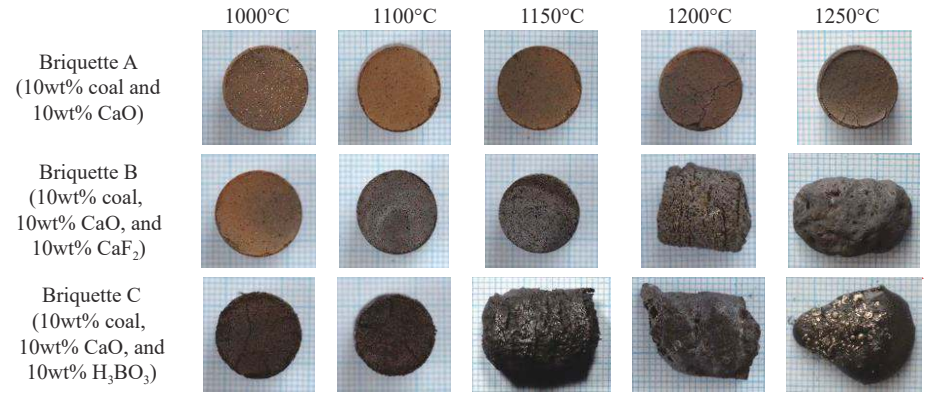

Fig. 5. Briquettes after the reduction process.

each experiment is shown in Fig. 6. The percentage of weight loss increased as the temperature rose due to the reduction of oxygen in the nickel ore by carbon in coal to produce ferronickel. Accordingly, the amount of ferronickel formation increased as the temperature increased. The weight loss percentages based on thermodynamic software FactSage 7.1 calculations were 17.83%–19.54% for briquette A, 17.83%–19.54% for briquette B, and 21.13%–25.56% for briquette C. The highest weight loss was associated with briquette C, which was due to the dissociation of H_3BO_3 into $H_2O(g)$, $B_2O_3(l)$, $(HBO_2)_3(g)$, and $H_3BO_3(g)$. The experimental results had similar trends to the thermodynamic calculation results.

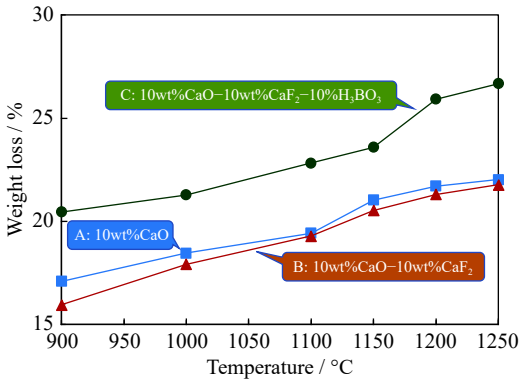

Fig. 6. Weight loss of briquettes after the reduction process.

3.3. Ferronickel particle size

Optical microscope observations on the surface of briquettes A, B, and C at 1100–1250°C are shown in Fig. 7. For briquette A, the metallographic preparation technique could only be applied to the reduced briquette from experiments at 1250°C. At temperature ≤ 1200°C, the samples were weak and difficult to be metallographically prepared for optical microscopy observation. In general, the ferronickel size in briquette C had large particles, followed by those in briquettes B and A. To determine the ferronickel particle sizes, five photographs from each briquette were obtained, and the particle sizes were quantified using ImageJ software. Given that the particles exhibited irregular shapes, the particle size was calculated based on the diameter of the spherical shape using the surface area data from ImageJ software. The results of ferronickel particle size quantification at 1250°C are depicted in Fig. 8, which shows the relationship between the number of particles and their sizes. All briquettes with a large number of ferronickel particles had particle sizes less than 10 μm. The maximum size of ferronickel particles in briquettes A, B, and C at reduction temperature of 1250°C were in the range of 20–30, 100–200, and 300–400 μm, respectively.

The particle size distributions of ferronickel in briquettes B and C at various reduction temperatures are summarized in Figs. 9 and 10, respectively. Increasing the temperature shifted the particle size distribution toward larger sizes. The number of particles less than 10 μm decreased with increasing temperature. At 1100°C, the maximum particle size for briquettes B and C was 20–30 μm. At 1150°C and above, the ferronickel particle sizes continued to grow. In general, the particle sizes in briquette C were larger than those in briquette B. In terms of thermodynamics, increasing the reduction temperature caused the Gibbs free energy to become more negative. The Gibbs free energy, which has a negative value, indicates a spontaneous reduction reaction. In terms of reaction kinetics, rising the temperature caused the reaction to occur faster. Furthermore, high temperatures provided additional liquid phase in the slag, which made the ferronickel particles move and agglomerate easily to form large particles.

The maximum sizes of ferronickel particles in briquettes A, B, and C at 900–1250°C are shown in Fig. 11. When the reduction temperature was raised from 1100 to 1250°C, the maximum particle size increased in briquettes B and C. A drastic increase in the maximum size of ferronickel occurred between 1200 and 1250°C for briquette B, which indicated a 117% growth (from 76 to 165 μm). By contrast, a drastic increase in maximum particle size in briquette C occurred between 1150 and 1200°C, which suggested a 427% growth (from 55 to 290 μm). From 1200 to 1250°C, the ferronickel particle size in briquette C increased by 29% (from 290 to

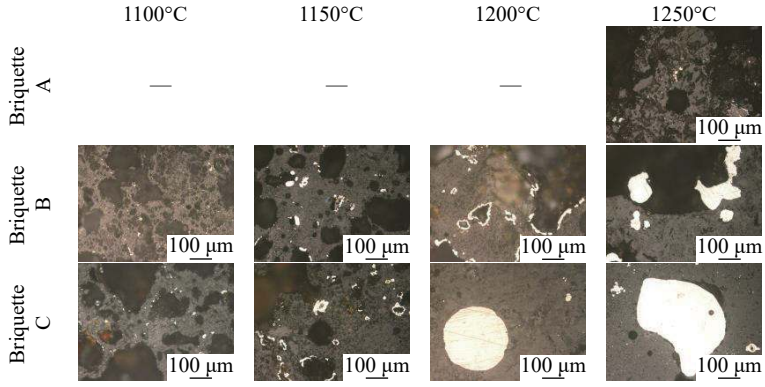

Fig. 7. Optical microscope observation of the briquettes after the reduction process with 200× magnification.

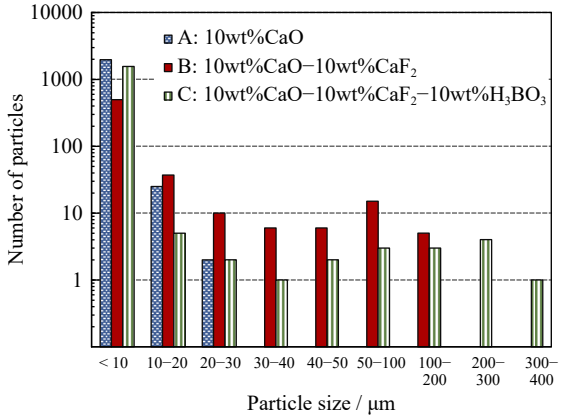

Fig. 8. Relationship between number of particles and particle size at 1250°C.

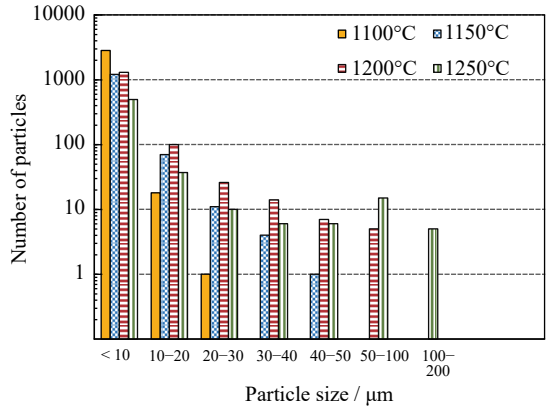

Fig. 9. Relationship between number of particles and particle size at 1250°C for briquette B (10wt%CaO–10wt%CaF_2).

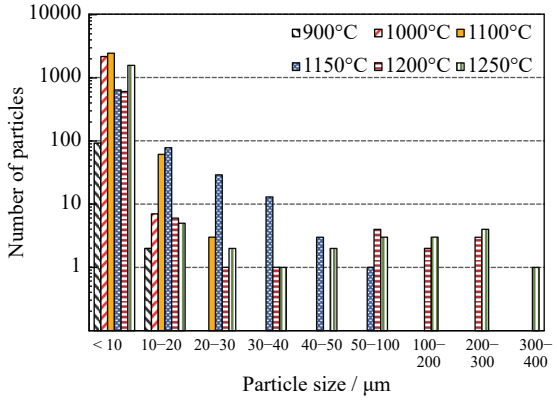

Fig. 10. Relationship between number of particles and particle size at 1250°C for briquette C (10wt%CaO–10wt%CaF_2–10wt%H_3BO_3).

376 μm).

Upon heating of saprolitic nickel laterite ore, mineral serpentine in the ore decomposes. At 750°C, serpentine dissociates into olivine and silica in accordance with the following reaction [8]:

$$2(Mg,Fe,Ni)_3Si_2O_5(OH)_4(s) = 3(Mg,Fe,Ni)_2SiO_4(s) + SiO_2(s) + 4H_2O(g) \quad (1)$$

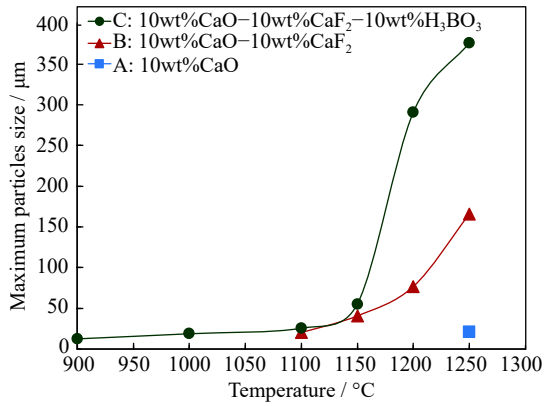

Fig. 11. Maximum particle size as a function of temperature and flux.

Olivine is a phase that is difficult to reduce and can inhibit the reduction of nickel and iron oxides. The addition of CaO to the saprolitic nickel laterite ore can reduce the melting point of slag. The addition of CaO can also exchange the NiO component in the olivine phase, leading to the facile reduction of NiO in the ore.

CaF_2 can reduce the melting point of slag during the reduction of saprolitic nickel laterite ore. The $SiO_2/(SiO_2 + MgO)$ ratio of the ore used in the present study was 0.67 (see Table 1). At this composition, thermodynamic calculations indicated that the melting point of slag was around 1600°C. When 10wt% CaF_2 was added, the thermodynamic calculation showed a decrease in the slag melting point to around 1200°C. The addition of 10wt% CaF_2 in briquette B allowed the formation of a liquid phase at low temperatures, enabling the production of large ferronickel particles.

The simultaneous addition of CaO, CaF_2, and H_3BO_3 to the saprolitic nickel laterite ore further lowered the slag melting point. During heating, boric acid underwent a gradual decomposition. This decomposition of H_3BO_3 produced boron trioxide (B_2O_3). Boron trioxide is an oxide compound that has a low melting temperature, which is around 450°C. The addition of boric acid to briquette C promoted the formation of a liquid phase at a low temperature compared with the two other briquettes. The higher the temperature, the more liquid phases formed.

3.4. Percentage of metal phase and chemical composition of metals

The percentages of metal phases of ferronickel particles in briquettes A, B, and C at various temperatures are shown in Fig. 12. The metal phase percentage was determined using ImageJ software. The metal phase percentage was calculated by dividing the surface area of metal phase with total surface area of the sample from the optical microscopy images. The metal phase percentages in briquettes B and C increased with increasing reduction temperatures. The highest metal phase percentage was produced from the reduction of briquette C at

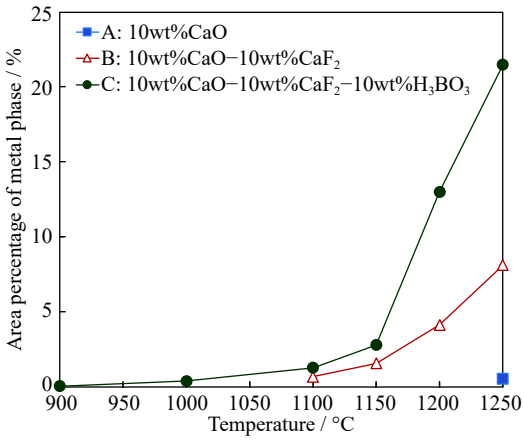

Fig. 12. Metal phase as a function of temperature and flux.

1250°C, i.e., 21.46%. The trend of the percentage of metal phases was similar to that of the maximum particle sizes (Fig. 11).

Liquid phase formation in slag at various temperatures and the mechanism of agglomeration of ferronickel particles have been described by Elliott *et al.* [8] and Rao *et al.* [12]. At the time of reduction, the presence of a liquid phase in slag caused the sintering of ferronickel particles through capillary forces between adjacent particles. The liquid phase in slag became a facility for small ferronickel particles to agglomerate into large particles. In general, increasing the reduction temperature can produce additional liquid phase as indicated by the thermodynamic calculations. The increase in liquid phase will encourage the agglomeration of particles to large sizes and raise the percentage of the metal phase.

The results of SEM–EDS observations on briquettes B and C after the reduction at 1250°C are shown in Figs. 13 and 14, respectively. Iron and nickel were accumulated in the ferronickel metals, whereas silicon, magnesium, and calcium were contained in the slag. The chemical compositions of ferronickel are given in Table 6. The carbon content in the briquette was not reported due to the inaccurate carbon determination in the present measurement. In general, the nick-

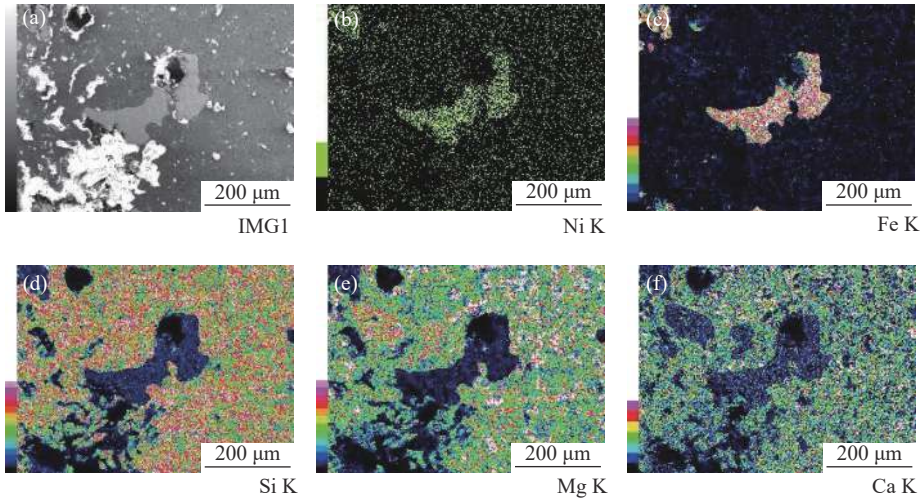

Fig. 13. SEM image (a) and EDS elemental mapping (b–f) of briquette B after reduction at 1250°C, 200× magnification.

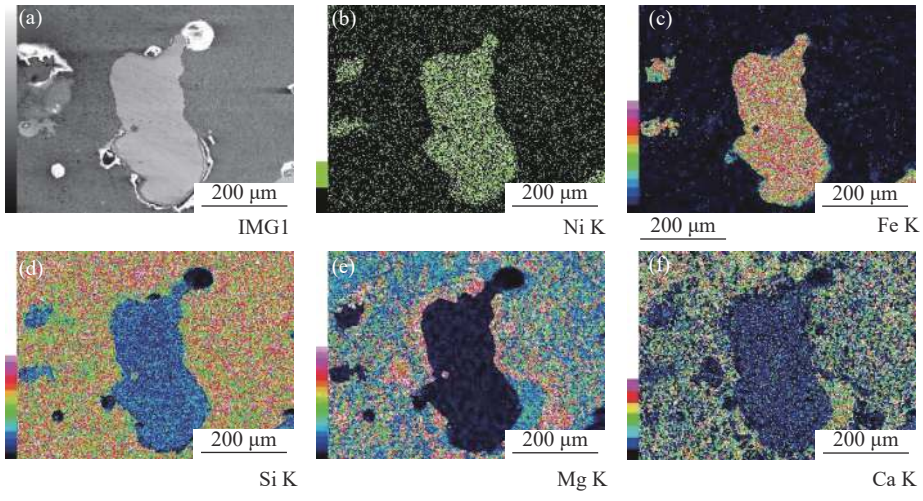

Fig. 14. SEM image (a) and EDS elemental mapping (b–f) of briquette C after reduction at 1250°C, 200× magnification.

el content in briquette C was higher than that in briquette B. The experimental data confirmed the thermodynamic calculation result. Thus, the addition of H_3BO_3 increased the nickel content in ferronickel and suppressed the reduction of iron oxide.

Table 6. Chemical composition of ferronickel determined by SEM–EDS wt%

Briquette	Ni	Fe	Si	Cr
B	7.91	88.52	0.71	2.76
C	8.59	85.65	3.52	2.25

The experimental results showed the feasibility of producing ferronickel particles with a large particle size at low temperatures through the modification of the slag by the addition of different additives. The large ferronickel particle size leads to better separation of metals from the unreduced components. The present study demonstrated the possibility of processing lateritic nickel ore at low temperatures, resulting in low energy consumption and low operational cost.

CaF_2 is not environmentally friendly, so the slag containing CaF_2 shall be treated and handled carefully. Furthermore, the volume of the produced slag may increase due to the presence of B_2O_3 with low density. Principally, this slag could be utilized as raw material for magnesium production. Magnesium metal can be recovered from ferronickel slag with a high recovery degree by the addition of calcium oxide [25]. The influence of CaF_2 and B_2O_3 on the recovery of magnesium from ferronickel slag should be further studied.

4. Conclusion

Low-grade saprolitic nickel laterite ore was reduced by 10wt% coal and additives. The addition of 10wt% CaO had a slight influence on the formation of ferronickel particles where the maximum particle size was 20 μm at 1250°C. The addition of 10wt% CaO and 10wt% CaF_2 into low-grade saprolitic nickel laterite ore increased the ferronickel particle size to 165 μm at 1250°C due to the increase in the liquid slag phase, which facilitated metal migration and agglomeration into large ferronickel particles. The addition of 10wt% CaO, 10wt% CaF_2, and 10wt% of H_3BO_3 resulted in a ferronickel particle size of 376 μm at 1250°C. The presence of boric trioxide (B_2O_3) further reduced the melting temperature of the slag. The presence of liquid phase in the slag and the large ferronickel size led to the separation of the ferronickel particles from the impurities.

Acknowledgements

The authors would like to thank the Program of Research, Community Service, and Innovation of the Institut Teknologi Bandung (P3MI–ITB) for funding this research.

References

[1] Team Kalkine, *How Is the Nickel Landscape Shaping Up*, Kalkine Media, Sydney [2019-11-13]. https://kalkinemedia.com/au/blog/how-is-the-nickel-landscape-shaping-up.

[2] U.S. Geological Survey, *Mineral Commodity Summaries 2019*, U.S.GeologicalSurvey,Washington[2019-02-28].https://doi.org/10.3133/70202434.

[3] C.T. Harris, J.G. Peacey, and C.A. Pickles, Thermal upgrading of nickeliferous laterites—A review, [in] J. Liu, J. Peacey, M. Barati, S. Kashani-Nejad, and B. Davis, eds., *Pyrometallurgy of Nickel and Cobalt 2009*, Proceedings of the 48th Conference on Metallurgists, Ontario, 2009, p. 51.

[4] J.C. Dong, Y.G. Wei, S.W. Zhou, B. Li, Y.D. Yang, and A. McLean, The effect of additives on Ni, Fe and Co from nickel laterite ores, *JOM*, 70(2018), No. 10, p. 2365.

[5] G.H. Li, T.M. Shi, M.J. Rao, T. Jiang, and Y.B. Zhang, Beneficiation of nickeliferous laterite by reduction roasting in the presence of sodium sulfate, *Miner. Eng.*, 32(2012), p. 19.

[6] D.Q. Zhu, Y. Cui, K. Vining, S. Hapugoda, J. Douglas, J. Pan, and G.L. Zheng, Upgrading low nickel content laterite ores using selective reduction followed by magnetic separation, *Int. J. Miner. Process.*, 106-109(2012), p. 1.

[7] D.Q. Zhu, L.T. Pan, Z.Q. Guo, J. Pan, and F. Zhang, Utilization of limonitic nickel laterite to produce ferronickel concentrate by the selective reduction–magnetic separation process, *Adv. Powder Technol.*, 30(2019), No. 2, p. 451.

[8] R. Elliott, C.A. Pickles, and J. Peacey, Ferronickel particle formation during the carbothermic reduction of a limonitic laterite ore, *Miner. Eng.*, 100(2017), p. 166.

[9] M. Jiang, T.C. Sun, Z.G. Liu, J. Kou, N. Liu, and S.Y. Zhang, Mechanism of sodium sulfate in promoting selective reduction of nickel laterite ore during reduction roasting process, *Int. J. Miner. Process.*, 123(2013), p. 32.

[10] J. Lu, S.J. Liu, J. Shangguan, W. Du, F. Pan and S. Yang, The effect of sodium sulphate on the hydrogen reduction process of nickel laterite ore, *Miner. Eng.*, 49(2013), p. 154.

[11] C.T. Harris, J.G. Peacey, and C.A. Pickles, Selective sulphidation and flotation of nickel from a nickeliferous laterite ore, *Miner. Eng.*, 54(2013), p. 21.

[12] M.J. Rao, G.H. Li, X. Zhang, J. Luo, Z.W. Peng, and T. Jiang, Reductive roasting of nickel laterite ore with sodium sulphate form Fe–Ni production. Part Ⅱ: Phase transformation and grain growth, *Sep. Sci. Technol.*, 51(2016), No. 10, p. 1727.

[13] X.P. Wang, T.C. Sun, C. Chen, and J. Kou, Effects of Na_2SO_4 on iron and nickel reduction in a high-iron and low-nickel laterite ore, *Int. J. Miner. Metall. Mater.*, 25(2018), No. 4, p. 383.

[14] G.J. Chen, J.S. Shiau, S.H. Liu, and W.S. Hwang, Optimal combination of calcination and reduction conditions as well as Na_2SO_4 additive for carbothermic reduction of limonite ore, *Mater. Trans.*, 57(2016), No. 9, p. 1560.

[15] S.W. Zhou, Y.G. Wei, B. Li, H. Wang, B.Z. Ma, and C.Y. Wang, Chloridization and reduction roasting of high-magnesium low-nickel oxide ore followed by magnetic separation to enrich ferronickel concentrate, *Metall. Mater. Trans. B*, 47(2016), No. 1, p. 145.

[16] Z.Z. Wang, M.S. Chu, Z.G. Liu, H.T. Wang, W. Zhao, and L.H. Gao, Preparing ferro-nickel alloy from low grade laterite nickel ore based on metallized reduction–magnetic separation, *Metals*, 7(2017), No. 8, p. 313.

[17] T. Watanabe, S. Ono, H. Arai, and T. Matsumori, Direct reduction of garnierite ore for production of ferro-nickel with a rotary

kiln at Nippon Yakin Kogyo Co., Ltd., Oheyama Works, *Int. J. Miner. Process.*, 19(1987), No. 1-4, p. 173.

[18] Y. Kobayashi, H. Todoroki, and H. Tsuji, Melting behavior of siliceous nickel ore in a rotary kiln to produce ferronickel alloys, *ISIJ Int.*, 51(2011), No. 1, p. 35.

[19] H. Tsuji, Behavior of reduction and growth of metal in smelting of saprolite Ni-ore in a rotary kiln for production of ferronickel alloy, *ISIJ Int.*, 52(2012), No. 6, p. 1000.

[20] A.E.M. Warner, C.M. Díaz, A.D. Dalvi, P.J. Mackey, and A.V. Tarasov, JOM world nonferrous smelter survey, Part Ⅲ: Nickel: Laterite, *JOM*, 58(2006), No. 4, p. 11.

[21] B. Li, H. Wang, and Y.G. Wei, The reduction of nickel from low-grade nickel laterite ore using a solid-state deoxidisation method, *Miner. Eng.*, 24(2011), No. 14, p. 1556.

[22] X.M. Lv, L.W. Wang, Z.X. You, J. Dang, X.W. Lv, G.B. Qiu, and C.G. Bai, Preparation of Ferronickel from Nickel Laterite Ore via Semi-Molten Reduction Followed by Magnetic Separation, [in] *Extraction 2018*, Cham, 2018, p. 913

[23] X.D, Ma, Z.X. Cui, and B.J. Zhao, Efficient utilization of nickel laterite to produce master alloy, *JOM*, 68(2016), No. 12, p. 3006.

[24] M.H. Morcali, L.T. Khajavi, and D.B. Dreisinger, Extraction of nickel and cobalt from nickeliferous limonitic laterite ore using borax containing slags, *Int. J. Miner. Process.*, 167(2017), p. 27.

[25] X. Zhang, F.Q. Gu, Z.W. Peng, L.C. Wang, H.M. Tang, M.J. Rao, Y.B. Zhang, G.H. Li, T. Jiang, and Y. Wang, Recovering magnesium from ferronickel slag by vacuum reduction: Thermodynamic analysis and experimental verification, *ACS Omega*, 4(2019), No. 14, p. 16062.